IN-34
117615
P-12

Navier-Stokes Turbine Heat Transfer Predictions Using Two-Equation Turbulence

Ali A. Ameri
Lewis Research Center
Cleveland, Ohio

and

Andrea Arnone
Institute for Computational Mechanics in Propulsion
Lewis Research Center
Cleveland, Ohio

N93-10735

Unclas

G3/34   0117615

(NASA-TM-105817)   NAVIER-STOKES
TURBINE HEAT TRANSFER PREDICTIONS
USING TWO-EQUATION TURBULENCE
(NASA)   12 p

NASA

ICOMP
NASA Lewis Research Center
Case Western Reserve University
Ohio Aerospace Institute
INSTITUTE FOR COMPUTATIONAL MECHANICS IN PROPULSION

NAVIER-STOKES TURBINE HEAT TRANSFER PREDICTIONS USING TWO-EQUATION TURBULENCE CLOSURES

Ali A. Ameri*†
Center for Research, Inc.
University of Kansas
Lawrence, Kansas

and

Andrea Arnone*
Department of Energy Engineering
University of Florence
Florence, Italy

ABSTRACT

Navier-Stokes calculations were carried out in order to predict the heat transfer rates on turbine blades. The calculations were performed using TRAF2D which is a two-dimensional, explicit, finite volume mass-averaged Navier-Stokes solver. Turbulence was modeled using Coakley's $q-\omega$ and Chien's $k-\epsilon$ two-equation models and the Baldwin-Lomax algebraic model. The model equations along with the flow equations were solved explicitly on a non-periodic C grid. Implicit residual smoothing (IRS) or a combination of multigrid technique and IRS was applied to enhance convergence rates. Calculations were performed to predict the Stanton number distributions on the first stage vane and blade row as well as the second stage vane row of the Rocketdyne Space Shuttle Main Engine (SSME) high pressure fuel turbine. The comparison with the experimental results, although generally favorable, serves to highlight the weaknesses of the turbulence models and the possible areas of improving these models for use in turbomachinery heat transfer calculations.

NOMENCLATURE

C	Axial chord
D	Leading edge circle diameter
Fr	Frossling number, $Nu_D/\sqrt{Re_D}$
k	Turbulent kinetic energy
ℓ	Turbulent length scale
M	Mach number
Nu	Nusselt number
p	Pressure

---

* Member AIAA
† Resident Research Associate, NASA Lewis research Center

Pr	Prandtl number
q	Variable in the $q-\omega$ equations $=\sqrt{k}$
Re	Reynolds number
S	Surface distance
St	Stanton number
t	Time
T	Temperature
Tu	Turbulence intensity
u	velocity vector
v^*	Shear velocity
y	Distance from a solid surface
y^+	Distance in wall coordinates, yv^*/ν

Greek Symbols

β	Inlet angle
γ	Specific heat ratio
ϵ	Turbulence dissipation rate
δ_{ij}	Kronecker delta
κ	Thermal conductivity of the fluid
μ	Viscosity
ν	Kinematic viscosity
ω	ϵ/k
ρ	Density

Subscripts

0	Total condition
1	Inlet condition
D	Diameter as characteristic length
n	Derivative normal to the surface
2	Exit condition
T	Turbulent quantity
w	Surface conditions (wall)

INTRODUCTION

Accurate prediction of the airfoil heat transfer rates is critical in the design of modern gas turbines. Performing this task is difficult by virtue of the very

complex flow phenomena present in such turbines. Effects such as turbulence or organized unsteadiness are modeled because they are impractical to directly simulate due to limitations on computer memory and speed. Algebraic models usually work well for two-dimensional shear flows in local equilibrium and their implementation is easy and economical. However, in general, it may not be enough to prescribe turbulent scales by algebraic formulas. The time and length scales are dependent on transport effects and therefore need to be found from transport equations. Two equation models strike a good balance between the complex multi-equation models which represent more of the physics of turbulence and the simpler models. The model equations in low Reynolds number models are solved through the buffer layer to the wall. Low Reynolds number two-equation models are able to mimic transition induced by the free-stream turbulence. As the cases considered herein included transition, this ability is investigated in this paper. The phenomenon of reversed transition or relaminarization can also be accounted for using these types of models[1]. The features relating to transition and relaminarization are particularly useful in three-dimensional calculations where it is difficult to take advantage of empirical relations for the location of the start and extent of transition. The empirical relations are also often determined for two-dimensional flows which may limit their range of applicability.

In the present work Coakley's $q - \omega$ [2] and Chien's [3] $k - \epsilon$ low Reynolds number two-equation models are used. Previous applications [4,5,6] of the models to the prediction of blade heat transfer have been reported. The above models were chosen for their good numerical convergence properties. The model equations were incorporated in a two-dimensional cascade analysis code. For the rotating blade, the flow was solved in the relative reference frame and the body forces were neglected. The code utilized was the TRAF2D(TRAnsonic Flow 2D)[7] code which is a compressible, mass-averaged, Navier-Stokes solver.

Shuttle Main Engine (SSME) high-pressure fuel turbine. Stanton number distributions were predicted for the first-stage vane and blade rows as well as the second-stage vane row. The results of the calculations were compared with the experimental measurements of Dunn and Kim [9] which were obtained using a short duration measurement technique.

DESCRIPTION OF THE ANALYSIS

The flow was modeled using mass-weighted compressible Navier-Stokes equations and perfect gas equation of state. The variation of viscosity with temperature was assumed to follow Sutherland's law[10]. The effect of turbulence was modeled using two low Reynolds number two-equation models. Solutions using the Baldwin-Lomax algebraic model were also generated for comparison.

Turbulence Models

The turbulence was modeled using two-equation, low-Reynolds number turbulence models. Transition to turbulence is automatically mimicked by such models. Chien's $k - \epsilon$ and Coakley's $q - \omega$ models were chosen for this work. The general formulation of the two models is written below following [2]:

$$(\rho s_i)_t + (\rho s_i u_j + q_{ij})_j = H_i$$

$$q_{ij} = -(\mu + \mu_t/Pr_i)s_{i,j} \ , \qquad i = 1, 2 \qquad (1)$$

For Chien's model the variables s_1 and s_2 are:

$$s_1 = k = q^2 \ , \quad s_2 = \epsilon = \omega k$$

$$\mu_T = C_\mu D \rho k/\omega$$

The Reynolds stresses can be calculated from:

D, E and F are damping functions

$$D = 1. - exp(-0.0115y^+), \qquad E = 1. - \frac{2}{3}exp[\frac{-R_T^2}{36}],$$

$$F = exp(-0.5y^+)$$

and

$$R_T = \frac{k}{\nu\omega}$$

also,

$Pr_k = 1.0$, $Pr_\epsilon = 1.3$, $C_\mu = 0.09$, $C_1 = 1.35$, $C_2 = 1.8$

For the $q - \omega$ model,

$$s_1 = q , \quad s_2 = \omega$$

$$\mu_T = C_\mu D\rho k/\omega$$

The source terms in the model equations are:

$$H_q = \frac{1}{2}[C_\mu DS/\omega^2 - \frac{2}{3}\mathcal{P}/\omega - 1]\rho\omega q \qquad (4)$$

$$H_\omega = [C_1(C_\mu S/\omega^2 - \frac{2}{3}\mathcal{P}/\omega) - C_2]\rho\omega^2$$

D is a damping function defined as:

$$D = 1. - exp(-\alpha R)$$
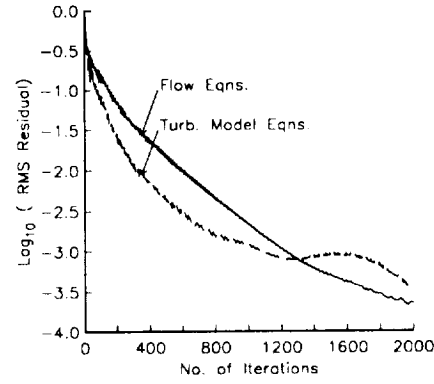
Figure 1: Convergence history- $q - \omega$ model, 2 levels of multigrid

Where Tu is the intensity of turbulence at the inlet of the computational domain and u_1 is the inlet velocity. The value of ϵ at the inlet is specified using the following relationship:

$$\epsilon = \omega k = k^{3/2}/\ell$$

where ℓ is the turbulence length scale representing the size of the energy containing eddies. This length scale is usually not reported as a part of the experimental conditions. For cascade conditions the length scale is assumed to be equal to a certain percent of the pitch. For example Hah [11] assumed a length scale equiva-
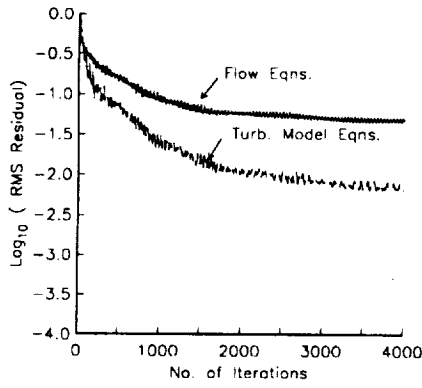
Figure 2: Convergence history- $q - \omega$ model, without multigrid

Figure 3: Convergence history- $k - \epsilon$ model

terms were needed for the model equations. Variable coefficient implicit residual smoothing was adapted to the model equations by setting up the coefficients using the eigenvalues of the model equations. This allowed larger CFL numbers and therefore faster convergence rates. A CFL number of 5.0 was used for all the calculations except for $k - \epsilon$ model's equations for which the CFL was in the range of 1.25-2.5. For the $q - \omega$ model, it was possible to extend the multigrid capability of the code to the model equations. Addition of second order dissipation terms was found to be unnecessary on the coarse grid for the model equations. Figures 1 and 2 show the convergence history for the $q - \omega$ model with and without multigrid. Figure 3 shows the convergence history for a calculation performed using Chien's model. The ordinate in those figures is the logarithm of the square root of the sum of the squares of the residuals over all the grid points divided by the number of grid points. The calculations were done for the first stage vane to be discussed later. The convergence history varies with varying values of exit Mach number and number of grid points among other factors.

Computational Grid

The discretization was performed on a non-periodic, C grid [7] generated by using a modified version of the Grape [14] code. With this type of grid the number of grid points on the suction surface of the airfoil is different than that on the pressure surface which leads to a much less skewed grid construction.

CPU Requirements

The CPU requirement per iteration per grid point was approximately 5.0E-5 second for the Baldwin-Lomax calculations with two levels of multigrid, 3.2E-5
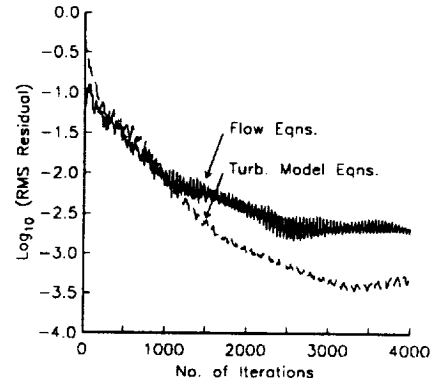
second for the $q - \omega$ runs with one level of multigrid and 5.0E-5 second for the Chien's model runs. The number of iterations needed was approximately 500, 2500 and 4000 for the above models respectively.

RESULTS AND DISCUSSION

The Stanton number is defined as:

$$St = \frac{-\kappa \frac{\partial T}{\partial n}|_{wall}}{\rho_{ref} C_p V_{ref}(T_w - T_0)} \qquad (5)$$

where T_w and T_0 are the wall temperature and the inlet total temperature respectively. ρ_{ref}, C_p and V_{ref} are the reference density, heat capacity and reference velocity. In the experiments the inlet to the first stage vane row is selected as reference.

Given the two-stage turbine overall pressure ratio, the pressure ratio across each row of airfoils is needed as input to the N-S solver. The pressure ratio across the row as well as inlet total pressure and temperature and the airfoil Reynolds number were taken from the MTSB [15] flow analysis code as provided by Boyle [16]. The experimental runs were made for two values of total pressure, resulting in two values of Reynolds number for each airfoil. Calculations were made for both values of Reynolds numbers. Table I contains the flow conditions of the turbine airfoils considered in this work. The free-stream turbulence levels for the three cascade rows are necessary for the calculations. The turbulence level upstream of the first stage vane was experimentally determined but was guessed for the other two cascade rows.

As stated earlier, the calculations were performed using the $q - \omega$ and Chien's $k - \epsilon$ two equation models as well as Baldwin-Lomax algebraic model. For the algebraic model the location of transition to turbulence on the two sides of the airfoil was specified to best fit the experimental results. It is worth mentioning that there are a host of empirical relations that can be used [17] to predict the start and the length of transition for use with algebraic models in two dimensions,
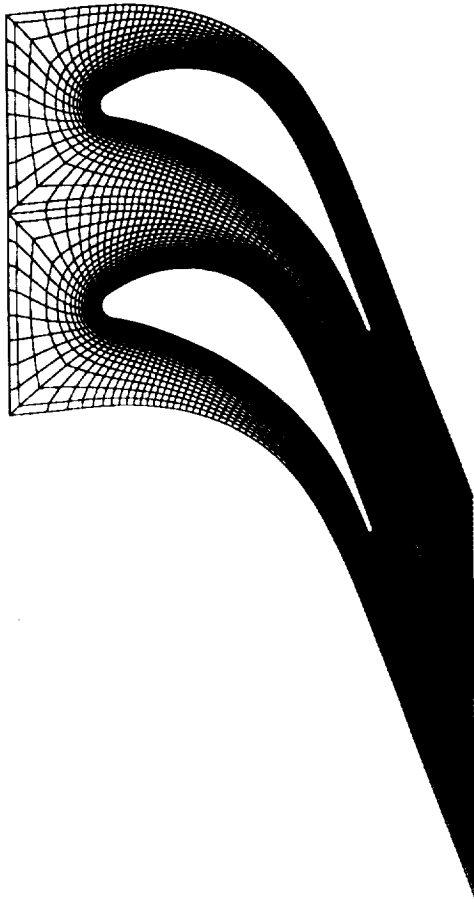
4

Figure 4: First stage vane and a typical grid

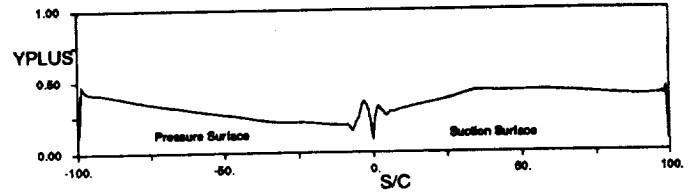however, that was not done here.

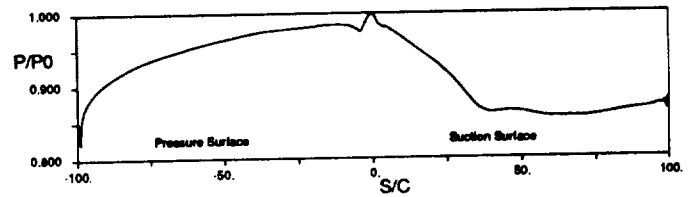Figure 5: Variation of the grid spacing from the wall in terms of y^+

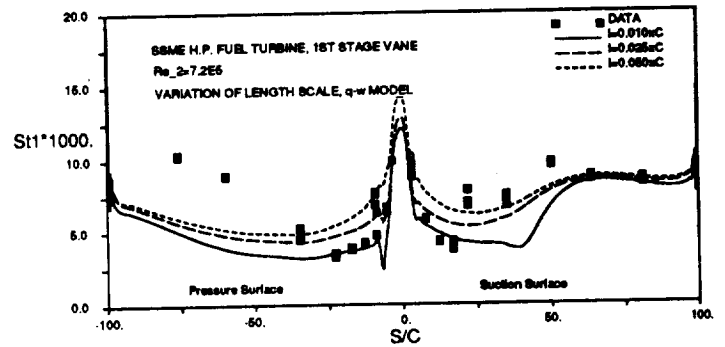Figure 6: Surface pressure distribution, first stage vane

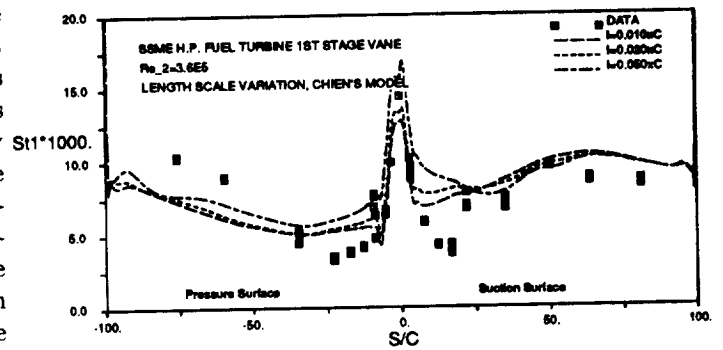Figure 7: Variation of St with length scale, $q - \omega$ model, $Re_2 = 3.6E5$

Figure 8: Variation of St with length scale, $k - \epsilon$ model, $Re_2 = 3.6E5$

First Stage Vane

Figure 4 shows the geometry of the first stage vane and the C grid generated. The mesh has 388x64 grid cells. The grid points are distributed such that there are 64 grid cells on the wake line on the pressure side of the airfoil and 32 grid cells on the wake line on the suction side. Figure 5 shows the distance of the first point away from the wall in terms of the dimensionless parameter y^+ on the first vane for the lower Reynolds number run. As can be seen, this value is consistently below unity. For the higher Reynolds number run the wall grid spacing was halved to keep the same y^+ distribution. Figure 6 presents the surface pressure distribution on the blade surface as a function of surface distance. On the suction side there is an initial region of favorable pressure gradient. The flow is likely to be laminar in this region for small values of free-stream turbulence. On the pressure side the flow encounters a small region of adverse pressure gradient following a short region of favorable pressure gradient. The adverse pressure gradient again can trigger transition for

5

	$P_0(psf)$	$T_0(^\circ R)$	β_1°	T_w/T_0	M_2	$Re_2 \times 10^{-5}$	$Tu\%$
1st STAGE VANE							

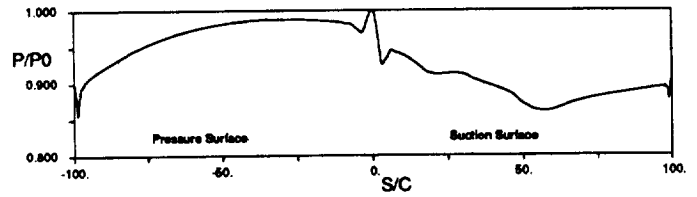Figure 11: First stage rotor blade and a typical grid

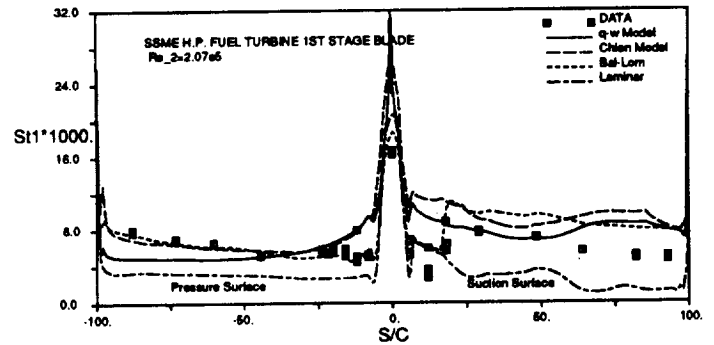Figure 12: First stage rotor, surface pressure distribution

Figure 13: First stage rotor, surface Stanton number, low Reynolds number

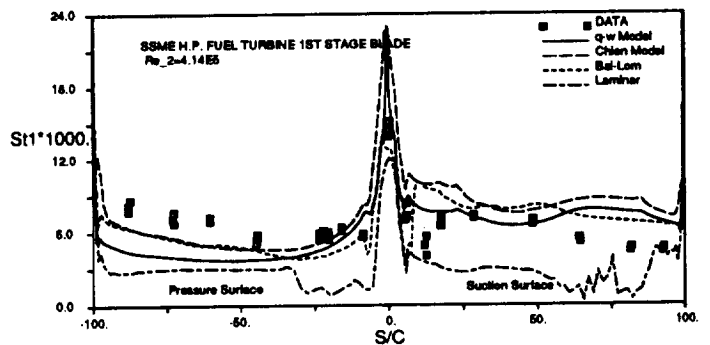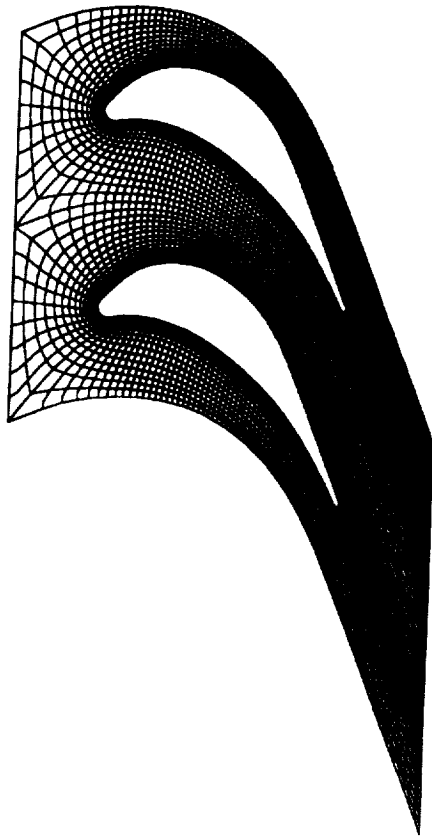Figure 14: First stage rotor, surface Stanton number, high Reynolds number

First Stage Blade

Figure 11 presents the rotor blade of the first stage of the SSME turbine at the midspan. The mesh has 388x64 grid cells. The grid points are distributed such that there are 64 grid cells on the wake line on the pressure side of the airfoil and 32 grid cells on the wake line on suction side. The same care regarding the grid resolution close to the wall was exercised when constructing the grid for this blade. Figure 12 is a plot of the surface pressure distribution as a function of the surface distance. Figures 13 and 14 compare the Stanton number results with the experimental results. The laminar flow calculation for the high Reynolds number separated on the suction side. The Frossling analysis yields values of 0.019 and 0.014 for the low and high Reynolds number stagnation point Stanton numbers, respectively. The corresponding experimental values are 0.016 and 0.015 resulting in Frossling numbers of 0.85 and 1.07. The location of transition on the suction surface is further upstream of the experimentally determined location. Referring to figures 12-14, both of the models predict transition on the suction side through the first adverse pressure gradient. The suction side level of Stanton number in the fully turbulent regime is correctly predicted for the low and the

7

Figure 15: Second stage vane and a typical grid

Figure 16: Second stage vane surface pressure
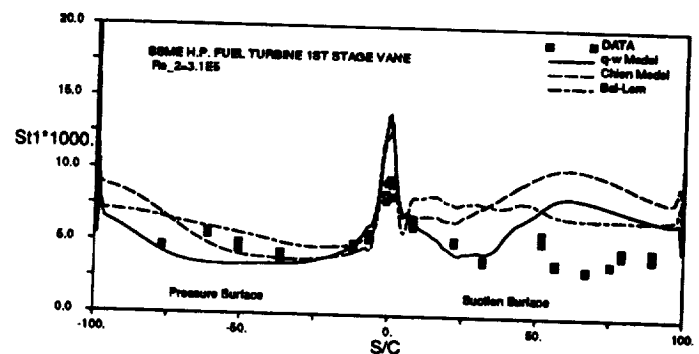
Figure 17: Second stage vane surface Stanton number, low Reynolds number

high Reynolds number cases with both of the models. On the pressure side, the $q - \omega$ model underpredicts the experimental Stanton number distribution. Chien's model and Baldwin-Lomax model both underpredict the pressure surface heat transfer for the high Reynolds number condition. Dunn et al. [19] numerically investigated the effect of surface roughness on the heat transfer characteristics of this blade since the blade surface was rough. They concluded that the surface roughness effect was limited to the high Reynolds number condition where there was a small effect on the pressure side and a 12% increase on the suction side.

Second Stage Vane

Figure 15 presents the geometry and a typical grid
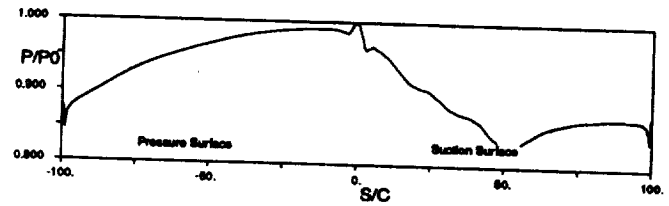constructed for the second stage

Reynolds number cases were calculated to be 0.0135 and 0.0096, respectively. The experimental measurements are smaller than the above results and yield Frossling numbers of 0.75 and 0.9 which are quite low in the highly turbulent environment of the vane. The transition process has been captured with the $q - \omega$ model, albeit not as well for the higher Reynolds number case. The $k - \epsilon$ model damped out the transition process, as was the case in the first vane. The data shows a phenomenon resembling a second transition process at the back of the blade on the suction surface which was not captured. The pressure side heat transfer results are satisfactory using both of the two-equation models although Chien's model's agreement with the experimental measurements is better.

SUMMARY AND CONCLUSIONS

Navier-Stokes calculations to obtain the Stanton number distribution on the airfoil surfaces of Rocketdyne SSME fuel high pressure turbine were performed. Coakley's $q - \omega$ and Chien's $k - \epsilon$ low Reynolds number turbulence models and the Baldwin-lomax algebraic models were used. The model equations were solved using an explicit scheme. It was possible to apply the multigrid technique to the solution of the $q - \omega$ model. Implicit residual smoothing was adapted to the solution of the equations for both of the two-equation models. Use of the above strategies helped to acceler-

REFERENCES

[1] W. P. Jones and B. E. Launder, "The Prediction of Laminarization with a Two-Equation Model of Turbulence," *International Journal of Heat and Mass Transfer.* 15:301 314, 1972.

[2] T. J. Coakley, "Turbulence Modeling Methods for the Compressible Navier-Stokes Equations." AIAA paper 83-1693, 1983.

[3] K. Y. Chien, "Prediction of Channel and Boundary-Layer Flows with a Low- Reynolds-Number Turbulence Model." *AIAA Journal.* 20:33 38, 1982.

[4] A. A. Ameri, P. M. Sockol and R. S. R. Gorla, "Navier-Stokes Analysis of Turbomachinery Blade External Heat Transfer," *AIAA Journal of Propulsion and Power.* 8:374 381, 1992.

[5] C. Hah, "Numerical Study of Three-Dimensional Flow and Heat Transfer near the Endwall of a Turbine Blade Row," AIAA paper 89-1689, 1989.

[6] C. A. Stephens and M. E. Crawford, "Investigation into the Numerical Prediction of Boundary-Layer

[14] R. L. Sorenson, "A Computer Program to Generate Two-Dimensional Grids about Airfoils and Other Shapes by the use of Poisson's Equation," NASA TM 81198, MAY 1980.

[15] R. J. Boyle, J. E. Haas and T. Katsanis, "Predicted Turbine Stage Performance Using Quasi-Three-Dimensional and Boundary-Layer Analyses," *AIAA Journal of Propulsion and Power*, 1(3):242,251, 1985.

[16] R. J. Boyle, NASA Lewis Research Center, Private communications.

[17] R. E. Mayle, " The Role of Laminar-Turbulent Transition in Gas Turbine Engines," *Journal of Turbomachinery*, Vol. 113:509–537, Oct. 1992.

[18] D. B. Taulbee, L. Tran and M. G. Dunn, "Stagnation Point and Heat Transfer for a Turbine Stage: Prediction and Comparison with Data," ASME paper 88-GT-30.

[19] M. G. Dunn, J. Kim, K .C. Civinskas and R. J. Boyle, "Time-Averaged Heat Transfer and Pressure Measurements and Comparison with Prediction for a Two-Stage Turbine," ASME Gas Turbine Conference, Cologne, Germany, June 1-4, 1992.

REPORT DOCUMENTATION PAGE

Form Approved
OMB No. 0704-0188

1. AGENCY USE ONLY *(Leave blank)*	2. REPORT DATE	3. REPORT TYPE AND DATES COVERED
	August 1992	Technical Memorandum

4. TITLE AND SUBTITLE

Navier-Stokes Turbine Heat Transfer Predictions Using Two-Equation Turbulence Closures

6. AUTHOR(S)

Ali A. Ameri and Andrea Arnone

5. FUNDING NUMBERS

WU–505–62–52

7. PERFORMING ORGANIZATION NAME(S) AND ADDRESS(ES)

National Aeronautics and Space Administration
Lewis Research Center
Cleveland, Ohio 44135–3191

8. PERFORMING ORGANIZATION REPORT NUMBER

E–7248

9. SPONSORING/MONITORING AGENCY NAMES(S) AND ADDRESS(ES)

National Aeronautics and Space Administration
Washington, D.C. 20546–0001

10. SPONSORING/MONITORING AGENCY REPORT NUMBER

NASA TM–105817
ICOMP–92–14

12a. DISTRIBUTION/AVAILABILITY STATEMENT

Unclassified - Unlimited
Subject Category 34

12b. DISTRIBUTION CODE

13. ABSTRACT *(Maximum 200 words)*

Navier-Stokes calculations were carried out in order to predict the heat transfer rates on turbine blades. The calculations were performed using TRAF2D which is a two-dimensional, explicit, finite volume mass-averaged Navier-Stokes solver. Turbulence was modeled using Coakley's q–ω and Chien's k–ε two-equation models and the Baldwin-Lomax algebraic model. The model equations along with the flow equations were solved explicitly on a non-periodic C grid. Implicit residual smoothing (IRS) or a combination of multigrid technique and IRS was applied to enhance convergence rates. Calculations were performed to predict the Stanton number distributions on the first stage vane and blade row as well as the second stage vane row of the Rocketdyne Space Shuttle Main Engine (SSME) high pressure fuel turbine. The comparison with the experimental results, although generally favorable, serves to highlight the weaknesses of the turbulence models and the possible areas of improving these models for use in turbomachinery heat transfer calculations.

14. SUBJECT TERMS

Navier-Stokes; Multigrid; Two equation model; Heat transfer

15. NUMBER OF PAGES

12

16. PRICE CODE

A03

17. SECURITY CLASSIFICATION OF REPORT	18. SECURITY CLASSIFICATION OF THIS PAGE	19. SECURITY CLASSIFICATION OF ABSTRACT	20. LIMITATION OF ABSTRACT
Unclassified	Unclassified	Unclassified	